Article ID 1672-6634(2018)01-0035-10 **DOI** 10.19728/j.issn1672-6634.2018.01.006

Extending the Responsive Spectrum Range of BiOCl Photocatalyst Through Rhodamine Sensitization and Its Photodegradation Performance Toward Phenol①

YANG Ya-nan ZENG Tian-tian HE Yin-na ZHANG Da-feng
PU Xi-peng MA Hui-yan

(School of Materials Science and Engineering, Liaocheng University, Liaocheng 252059, China)

Abstract BiOCl with different morphologies were synthesized by the hydrolysis of bismuth nitrate at different concentrations of NaOH solution. The structures, morphologies, and optical properties of the samples were studied by X-ray powder diffraction, scanning electron microscopy, ultraviolet-visible spectrophotometry and photoluminescence. Experimental results showed that the addition of NaOH can reduce the size of BiOCl sheets, and much more NaOH results in serious aggregation of BiOCl sheets. When 23 mmol NaOH was added into the solution, BiOCl showed the best adsorption ability and photocatalytic activity for Rhodamine (RhB) under visible light. Further, the responsive spectrum range BiOCl was further extended through RhB sensitization; and RhB sensitized samples show excellent photodegradation performance to phenol under visible light irradiation, but pure BiOCl exhibit poor photoactivity, suggesting that the photosensitization of RhB plays an important role in the reaction system. In addition, the main active species and the plausible photocatalytic mechanism were discussed in detail.

Key words BiOCl; photocatalyst; Rhodamine; sensitization; phenol

CLC number 643.36 **Document code** A

0 Introduction

Intense research in solarenergy conversion has been devoted in recent years due to concern of growing energy demands and increasing threats to the quality of human life due to environmental pollution[1,2]. Semiconductor-based photocatalysis has aroused broad because of its potential applicability in the fields of environmental pollutant removal, hydrogen generation from water and photoelectrochemical cells[3-6].

Titanium oxide (TiO_2) has been extensively studied because it is inexpensive, abundant and innocuous to the environment[7]. However, TiO_2 has a band gap of about 3.2 eV, and can only response to ul-

① 收稿日期:2017-10-19
基金项目:国家自然科学基金项目(51303076);山东省自然科学基金面上项目(ZR2018MEM019);大学生科技文化创新基金项目资助
通讯作者:蒲锡鹏,男,汉族,博士,教授,研究方向:新型能源材料,E-mail:puxipeng@lcu.edu.cn.

traviolet light irradiation, which limit its practically application[8]. Researchers proposed some methods to improve the photocatalytic activity of TiO_2, such as ion doping[9-11], noble metal decoration[12,13], dye sensitization[14] and constructing heterojunction with other semiconductor[15-17]. However, TiO_2 and TiO_2 based photocatalysts still show low photocatalytic activity in the wavelength range of visible light. Hence, researchers turn to develop new visible light photocatalysts.

The p-block photocatalyst BiOCl with a band gap of 3.4 eV exhibits high photocatalytic activity under ultraviolet light irradiation[18]. The special crystal structure of BiOCl results in an internal electric field, which contributes to the high separation efficiency of photoinduced electrons and holes[19]. Similarly, neat BiOCl photocatalyst shows low visible-light photocatalytic activity due to the large band gap and high recombination of photogenerated charges. Much effort has been made to extend the response spectrum of BiOCl to visible light range, such as controlling microstructure of BiOCl[20,21], ion doping[22,23] and dye sensitization[24,25]. Li and coworkers synthesized BiOCl with highly exposed (001) facets via a simple, fast and mild hydrothermal route using cationic polyacrylamide as both chlorine source and surfactant[20]. Li and coworkers reported that BiOCl photocatalysts doped with different contents of zinc were prepared via a facile ethylene glycol-assisted solvothermal process and showed good activity in photodecomposition of Rhodamine (RhB) under visible-light irradiation[26]. Cao group prepared Cu_2O/BiOCl photocatalyst with unique 3D/2D structure with enhanced visible-light photocatalytic activity[27].

As we all know, there is rare report on dye-sensitized BiOCl. Dye sensitization of semiconductor is an effective method to enhance the photodegradation ability[7,25]. Moreover, dye sensitized semiconductors can be used as in dye-sensitized solar cell, which is a potential way to convert solar energy. Mao and coworkers studied RhB-sensitized effect on the enhancement of photocatalytic activity of BiOCl toward bisphoenol-A under visible light irradiation. RhB, as a photosensitizer, can remarkably enhance the light utilization of BiOCl and the superior photocatalytic activity observed was attributed to the sensitization effect of RhB[25].

In this work, BiOCl was prepared through a hydrolysis method in the presence of NaOH, and as-synthesized BiOCl exhibit high adsorption ability. Further, the responsive spectrum range of samples was extended through RhB sensitization, leading to excellent photodegradation performance toward phenol, and the corresponding plausible mechanism was proposed.

1 Experimental

1.1 Synthesis processing

All reagents of analytical grade were obtained from Sinopharm Chemical Reagent Co. (Shanghai, China) and used without further purification. BiOCl was synthesized by the hydrolysis method of bismuth nitrate. First, 0.01 mol bismuth nitrate pentahydrate ($Bi(NO_3)_3 \cdot 5H_2O$) was dissolved in 20 mL deionized water under vigorous stirring for 10 min. Secondly, KCl (0.01 mol) and different amount of NaOH were dissolved in 20 mL deionized water under stirring, and the transparency solution was added dropwise to the $Bi(NO_3)_3$ solution followed by 30 min stirring. Finally, the white precipitate was filtered, washed with deionized water and absolute ethanol for several times, dried at 90℃ for further characterization. In order to modulate the hydrolysis of $Bi(NO_3)_3$, different amounts of NaOH of 0, 10, 20, 23, 25 and 33 mmol were used, and corresponding samples were labeled as BOC-0, BOC-10, BOC-20, BOC-23, BOC-25 and BOC-33, respectively. RhB-BOC-23 was prepared as follows: BOC-23 (0.1

g) was dispersed in 100 mL aqueous solution of RhB (20 mg/L). The suspension was treated by ultrasonic wave in dark for 30 min, then the purplish red catalyst was collected and washed with deionized water for several times, and then dried at 90℃.

1.2 Characterization

X-raydiffraction (XRD) patterns were recorded on a diffractometer (D8 Advanced, Bruker Co., Germany) with Cu Ka-radiation operated at 40 kV and 30 mA. The data were recorded in a 2θ range of 10°-80° with a step width of 0.02°. Scanning electron microscopy (SEM) was performed with a Gemini microscope (Zeiss Ltd., Germany). The Brunauer-Emmett-Teller (BET) specific surface areas of the samples were investigated by a Quantachrome Autosorb IQ-C nitrogen adsorption apparatus (Quantachrome Co., USA). Ultraviolet-visible (UV-vis) diffuse reflectance spectra (DRS) of samples and the adsorption spectra of RhB solution were measured by a UV-3600 spectrophotometer (Shimadzu Co., Japan). Photoluminescence (PL) spectra of the as-prepared samples were measured by an F-7000 spectrometer (Hitachi Ltd., Japan). The photocurrent analysis was carried out on an CHI-660C electrochemical workstation (Chenhua Co., China). ITO glass coated with the as-prepared samples served as the working electrode. A 0.1 M Na_2SO_4 aqueous solution was used as electrolyte.

1.3 Photocatalytic test

The photocatalytic activity of the prepared BiOCl catalyst toward RhB was evaluated, using 300 W Xenon lamp (CEL-HXF300) with a UV cutoff filter (JB450) as a visible light source with an intensity of 484 mW/cm^2. The lamp was positioned about 10 cm over a cylindrical container with a circulating water jacket for cooling (20℃). RhB was selected as a model pollutant to evaluate the photocatalytic activities of the as-prepared samples. Solid catalyst (0.1 g) was dispersed in 100 mL aqueous solution of RhB (20 mg/L). The solution was treated by ultrasonic wave in dark for 30 min to obtain a good dispersion and establish adsorption-desorption equilibrium between the organic molecules and the catalyst surface. Decrease in the concentration of RhB solution was analyzed by recording the adsorption band maximum (554 nm) in the adsorption spectra and taken as the initial concentration (C_0). During the photocatalysis, 5 mL of the suspension was extracted at an interval of 1 min, and the adsorption was measured after 3 min of centrifugation. The normalized temporal concentration changes (C/C_0) of RhB were obtained. The photocatalytic activity of RhB-sensitized BiOCl catalyst toward phenol (20 mg/L) was also evaluated at the same conditions. The characteristic adsorption of phenol at 276 nm was measured to monitor photocatalytic degradation.

2 Results and discussion

2.1 Characterization of samples

The XRD patterns of as-synthesized BiOCl are shown in Fig. 1(a). Obviously, all of the diffraction patterns can match well the tetragonal BiOCl (JCPDS No. 06-0249), and no other peaks of impurity phase are observed. Moreover, a gradual increase in the full width at half maximum is observed with increasing amount of NaOH. Using JADE software, the crystal sizes of BOC-0, BOC-10, BOC-20, BOC-23, BOC-25 and BOC-33 were calculated to be 39.2 nm, 35.5 nm, 27.5 nm, 22.9 nm, 19.4 nm and 14.9 nm, respectively. Fig. 1(b) shows the XRD patterns of BOC-23 and RhB-BOC-23. There is almost no different between the two diffraction profiles, indicating that RhB adsorption on the surface of BiOCl has no influence on the crystal structure of BiOCl.

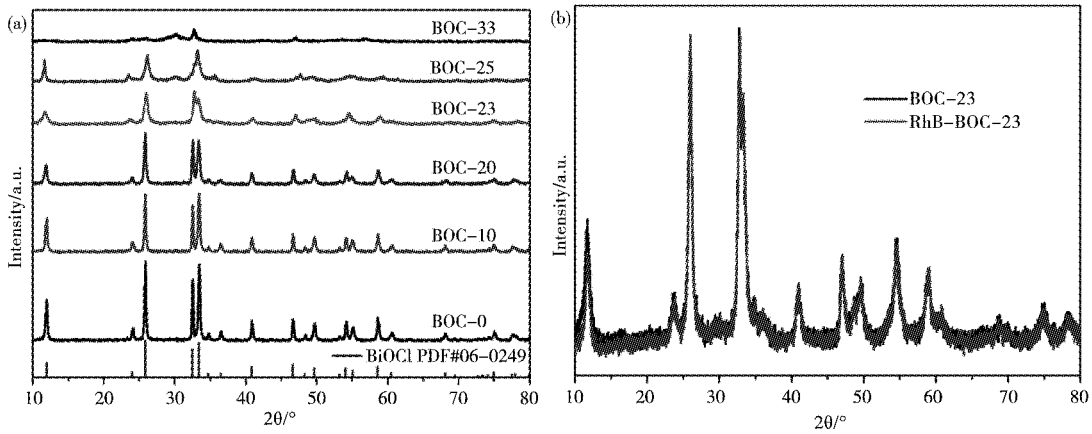

Fig. 1 (a) XRD patterns of as-synthesized samples using different NaOH amounts; (b) Comparison of patterns of BOC-23 and RhB-BOC-23

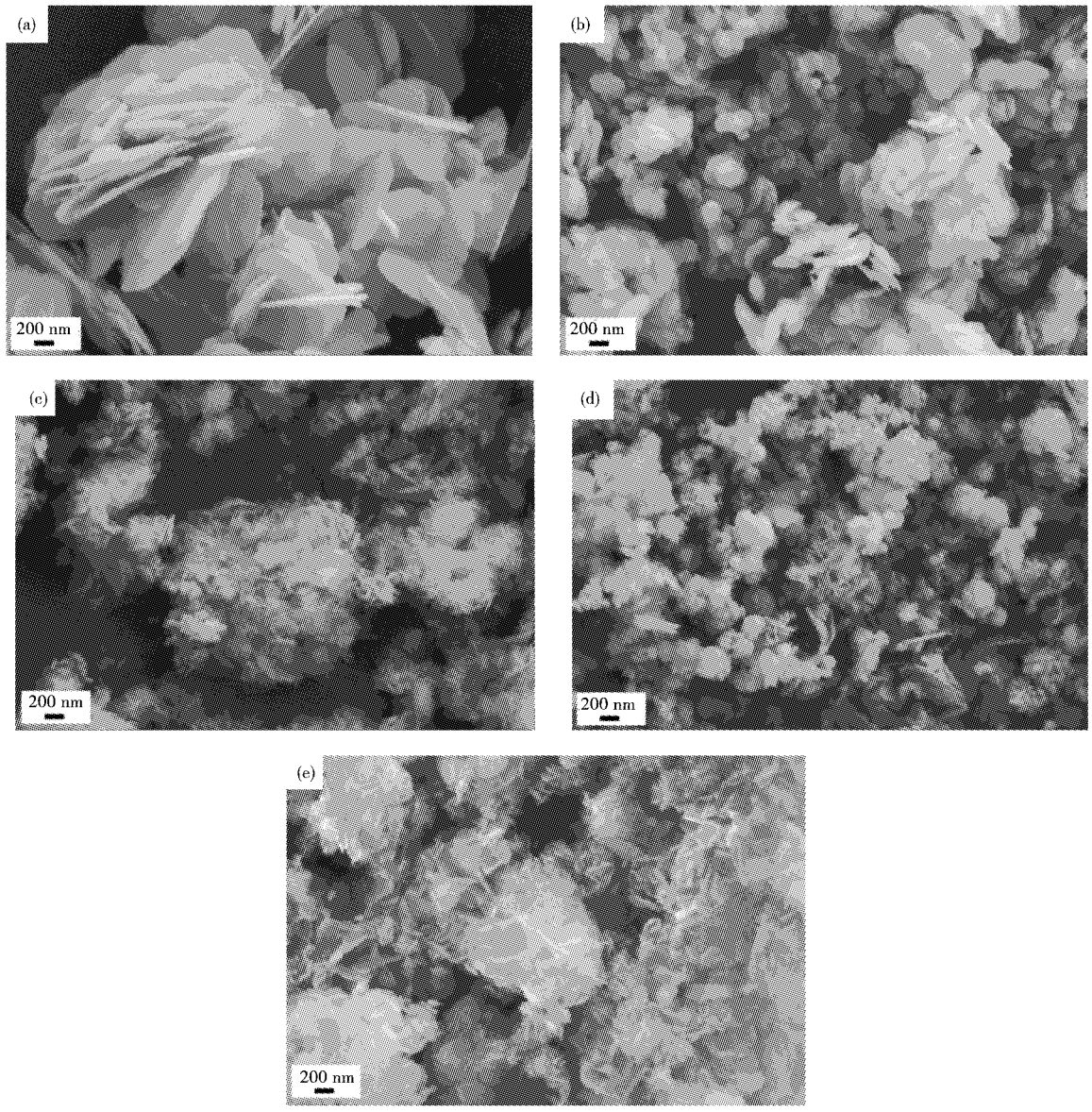

Fig. 2 SEM images of (a) BOC-0, (b) BOC-10, (c) BOC-23, (d) BOC-25, (e) BOC-33

The morphologies of as-prepared BiOCl photocatalysts were characterized by SEM, as shown in

Fig. 2. All samples are composed of sheets and aggregation of those. In addition, the size and thickness of sheets decrease significantly with increasing NaOH amount, which is in accordance with the above-mentioned XRD results. Especially for BOC-33, the sheets are so thin that wrinkles can be observed. However, larger NaOH amount can lead to serious aggregation of BiOCl sheets, as shown in BOC-33. The results suggest that NaOH plays a crucial role in the hydrolysis reaction of $Bi(NO_3)_3$ and the growth of BiOCl crystal. The BET areas of BOC-0, BOC-10, BOC-20, BOC-23, BOC-25 and BOC-33 were further characterized and are 16.19, 18.72, 22.45, 28.29, 30.41 and 24.56 m^2/g, respectively. The gradual increase in BET area with the increase of NaOH agrees well with the result of SEM.

Fig. 3(a) indicates the UV-vis DRS spectra of as-synthesized samples. The samples from BOC-0 to BOC-23 reveal an almost same adsorption edge of 360 nm with a tail extending to 400 nm, suggesting that both of them are obviously inactive in the visible-light range. Comparatively, for BOC-25 and BOC-33, the adsorption band shift to longer wavelength, indicating their visible light response were improved. As discussed in the XRD section, BOC-25 and BOC-33 are not well crystallized and exhibit poor photocatalytic activities, which leads to much more surface defects which will be discussed in detail in the following photocatalytic performance section. Due to the indirect nature of BiOCl, the band gaps (Eg) of samples were calculated following the equation: $(\alpha h\upsilon)^{1/2}=B(h\upsilon-Eg)$, where α, $h\upsilon$, Eg, and B are the adsorption coefficient, photon energy, band gap, and a constant, respectively[28]. The Eg values of as-synthesized samples can be estimated from Tauc plots of $(\alpha h\upsilon)^{1/2}$ versus the photon energy ($h\upsilon$), as shown in Fig. 3(b). The band gap (Eg) from BOC-0 to BOC-23 was almost same and determined to be 3.25 eV. However, the Eg of BOC-25 and BOC-33 are estimated to be 3.0 eV and 2.25 eV, respectively. The light absorption of RhB-BOC-23 was also characterized. Comparison with BOC-23, after RhB sensitization, RhB-BOC-23 shows much wider absorption range with a new adsorption band centered at 567 nm, due to the sensitization of RhB molecules[29]. The extended responsive spectrum rang has a beneficial effect on the effective utilization of visible light and thus excellent photoactivity.

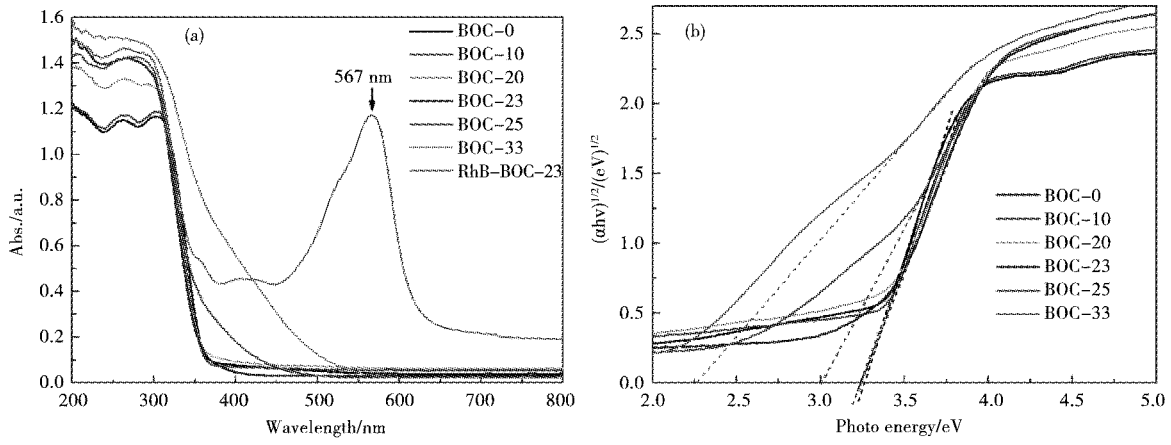

Fig. 3　(a) DRS spectra and (b) corresponding plots of $(ahn)^{1/2}$ versus photon energy (hn) of as-synthesized BiOCl and RhB-BOC-23

Fig. 4(a) shows thePL spectra of BOC-23 and RhB-BOC-23 upon 320 nm excitation, which provides information on the separation efficiency of photogenerated electron-hole (e^--h^+) pairs in photocatalysts. The emission band intensity of RhB-BOC-23 is significantly smaller than that of BOC-23, and this implies that RhB-BOC-23 has a more efficient separation of e^--h^+ pairs than BOC-23. To further probe the charge carrier separation and transportation, photocurrents of RhB-BOC-23 and BOC-23 were examined under simulated sunlight irradiation, as shown in Fig. 4(b). As expected, RhB-BOC-23 showed the higher photocurrent intensity compared with BOC-23, suggesting a higher separation effi-

ciency of the photoinduced electron-hole pairs due to the RhB sensitization[30].

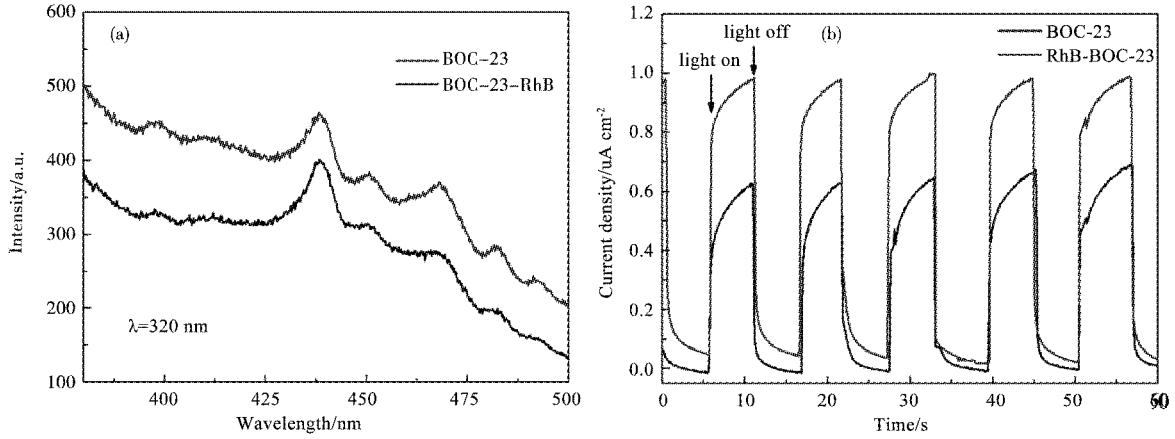

Fig. 4 (a) PL spectra upon 350 nm excitation; (b) Photocurrent density curves of BiOCl and RhB-BiOCl-23

2.2 Photocatalytic performance

Photocatalysis occurs predominantly on the catalyst surface so that the adsorption properties of photocatalysts have great influence on their photocatalytic activities. The adsorption properties of as-synthesized samples for RhB were characterized in dark, as shown in Fig. 5. Obviously, the adsorption/desorption equilibration can be established in 30 min, which ensures that adsorption has no contribution to the decoloration of RhB solution in the following photodegradation process. Moreover, it is found that BOC-23 shows the best adsorption properties and 90% of RhB molecules were adsorbed by the BOC-23 photocatalyst before photodegradation. The enhanced adsorption property can accelerate the diffusion of dye molecules from solution to the surface of photocatalysts, and thus speeds up the photocatalytic reaction[31].

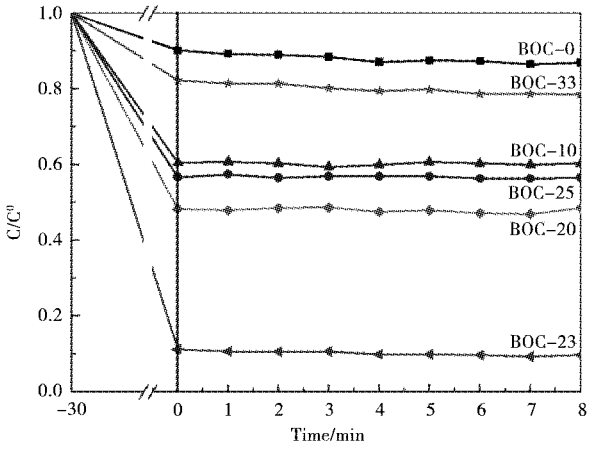

Fig. 5 The adsorption curves of as-synthesized samples for RhB

The combined adsorptive and photocatalytic degradation of RhB over the BiOCl photocatalyst are shown in Fig. 6(a). It is obvious that the concentration of RhB without photocatalyst samples has almost no change with increasing visible light irradiation time, which indicates RhB cannot be self-degraded in the following photodegradation test. As shown in Fig. 6(b), with increasing NaOH amount, the photocatalytic performance of samples increases first and then decreases significantly. BOC-23 exhibits the best photoactivity, and this can be explained by its high BET areas, which can provide more active sites in BOC-23, resulting in good adsorption ability and the best photodegradation performance. According to the DRS results, BiOCl has poor visible-light absorption, so that the photodegradation of RhB under visible light can be attributed to RhB sensitization[8,32]. In addition, although the BOC-25 and BOC-33 has smaller Eg, the surface defects act as recombination centers of photoinduced e^--h^+ pairs, resulting in poor photoactivity[33,34]. In order to improve the photoactivity of BiOCl, the sample BOC-23 was sensitized by RhB. And RhB-sensitized BOC-23 was further used to photodegrade phenol, as shown in Fig. 6(c). RhB-BOC-23 exhibited much better visible light photocatalytic activity of phenol than BOC-23 by a factor of 8.1, due to the extended re-

sponsive spectrum range after RhB sensitization. The photostabilities of BOC-23 and RhB-BOC-23 were investigated by cycling photocatalytic experiments, as shown in Fig. 6(d). In the six-run cycling test, the photodegradation performance of BOC-23 toward RhB only displays slight deterioration. Moreover, as shown in Fig. 6(e), the XRD patterns before and after cycling test have no changes, indicating the good photostability of BOC-23. However, in Fig. 6(f), the obvious deterioration of photodegradation performance toward phenol was observed in the cycling test of RhB-BOC-23, which can be attributed to the degradation of RhB molecules in the surface of BiOCl during the photocatalysis.

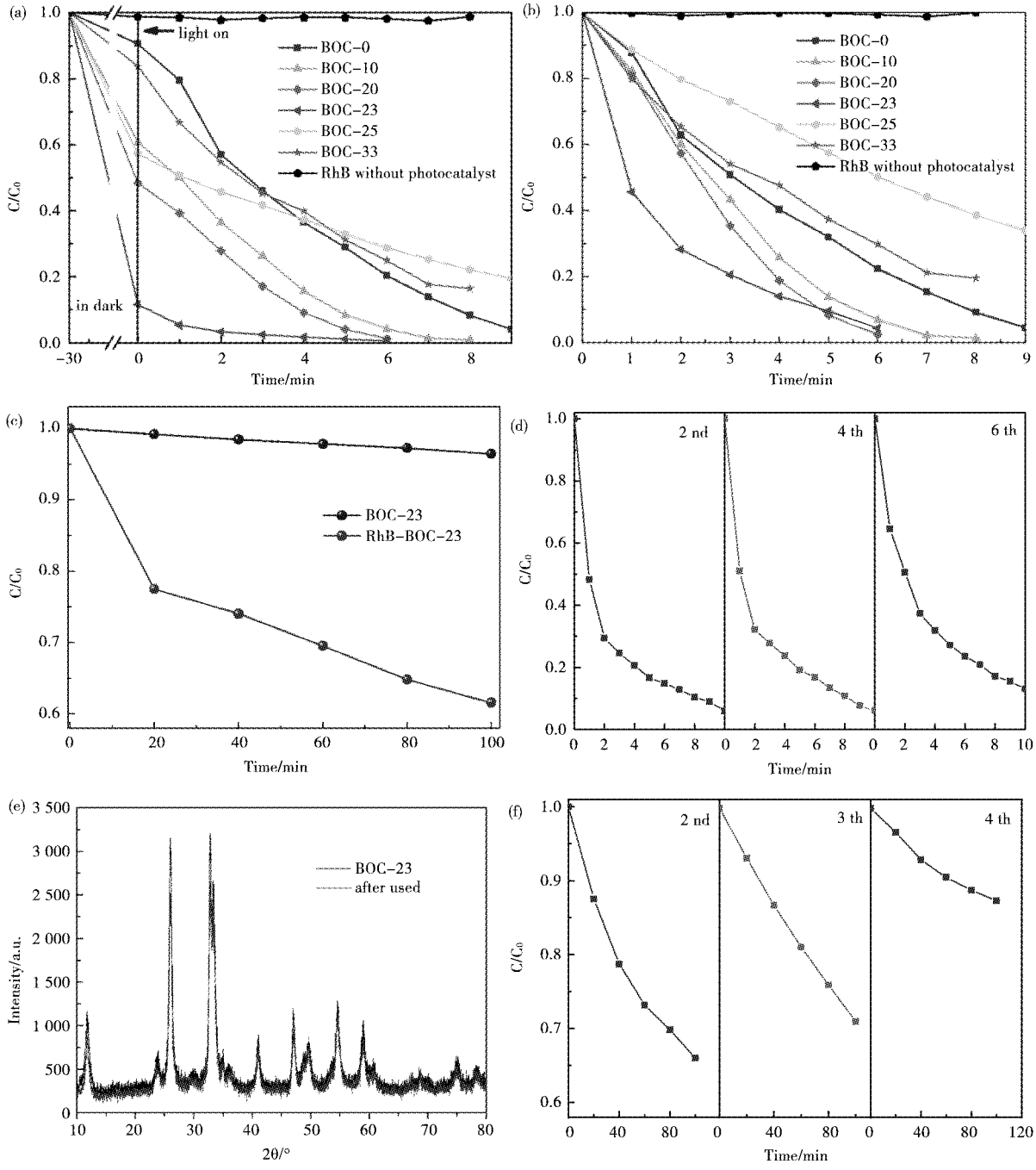

Fig. 6　(a) and (b) photodegradation curves of RhB for as-synthesized samples, (c) photodegradation curves of phenol for BOC-23 and RhB-BOC-23, (d) the stability test in photocatalytic degradation of RhB over BOC-23, (e) comparison of XRD patterns of BOC-23 before and after used. (f) The stability test in photocatalytic degradation of phenol over RhB-BOC-23

2.3 Photocatalytic mechanism

To understand the possible photocatalysis mechanism of BiOCl, the scavenger experiments were carried out to probe the main reactive species for the photocatalytic degradation. Three reagents of p-benzoquinone (BZQ), disodium ethylenediaminetetraacetate (Na_2-EDTA) and isopropyl alcohol (IPA) were chosen to be trap reagents for superoxide radicals ($\cdot O_2^-$), holes (h^+) and hydroxyl radicals ($\cdot$OH), respectively[35]. As shown in Fig. 7, in the presence of 1 mmol of IPA as a scavenger for $\cdot$OH radical species, no deterioration in photodegradation performance was found. However, when 1 mmol of Na_2-EDTA (h^+ scavenger) or 1 mmol BZQ ($\cdot O_2^-$ scavenger) was added, the degradation of RhB was significantly suppressed. The results indicate that h^+ and $\cdot O_2^-$ radical, rather than $\cdot$OH, are dominant active species in the photocatalytic reaction.

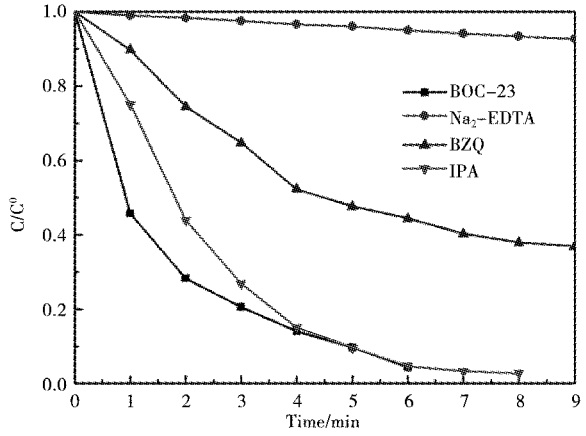

Fig. 7 Photocatalytic activities of BOC-23 in the presence of different trap reagents

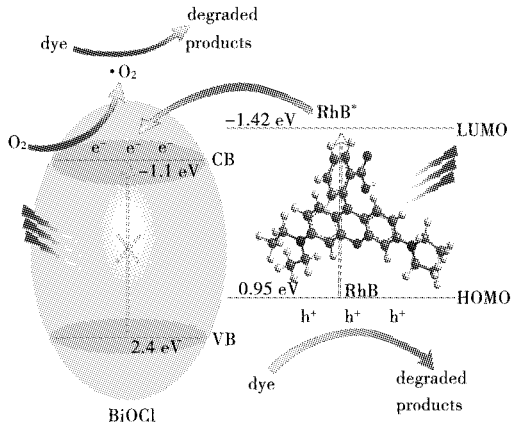

Fig. 8 Photocatalytic mechanism scheme of RhB-sensitized BiOCl under visible light irradiation

Based on the above results and discussion, the mechanism of photocatalytic activity enhancement for BiOCl was proposed and depicted in Fig. 8. The position of conduction band (CB) and valence band (VB) of BiOCl are −1.1 eV and 2.4 eV, respectively[36]. Hence, BiOCl with a wide band gap (Eg= 3.5 eV) is inert to visible light so that holes and electrons cannot be generated in BiOCl. However, RhB dye adsorbed on the BiOCl surface could be easily excited to be [RhB*] by the action of a visible light photon (l around 554 nm) so that RhB-sensitized BiOCl can response to visible light as shown in Fig. 3. The redox potentials of RhB (HOMO) and RhB* (LUMO) are 0.95 eV and −1.42 eV (vs. NHE), respectively[37]. As shown in Fig. 8, the LUMO of RhB is negative than CB of BiOCl so that RhB can used as the sensitization of BiOCl. Under the visible light irradiation, the photo-exited electrons generated from the adsorbed RhB are able to be injected into the CB of BiOCl. The electrons can react with dissolved oxygen in the solution to produce the reactive superoxide radical ($\cdot O_2^-$), leading to the photodegradation of dye molecules. Meanwhile, holes are generated in the HOMO of RhB and further degrade dye molecules. RhB sensitization of BiOCl shows excellent photocatalytic activity under visible light irradiation, which contributes to improving utilization of solar energy.

3 Conclusions

BiOCl photocatalysts were synthesized through the hydrolysis of bismuth nitrate. NaOH was added into the solution to modulate the hydrolysis process. The experimental results show that the addition of NaOH plays crucial roles in the morphologies of samples. With increasing amount of NaOH, the size and thickness of BiOCl sheets decreases gradually, and overmuch NaOH can result in serious aggrega-

tion of BiOCl sheet. BOC-23 exhibits the best adsorption ability and thus the best photodegradation performance for RhB under visible light irradiation. The improved photoactivity of as-synthesized BiOCl can be ascribed to the RhB sensitization effect. According to the DRS results, RhB-sensitized BiOCl can response to visible light of 567 nm so that RhB sensitization can broaden the light-responsive wavelength range of BiOCl photocatalyst. Consequently, RhB-sensitized BOC-23 exhibits improved photoactivity for phenol under visible light irradiation, which further confirms the RhB sensitization effect. Additionally, the hole and $\cdot O_2^-$, rather than $\cdot OH$, are dominant active species in the photocatalytic reaction.

References

[1] Al-Hetlani E, Amin M O, Madkour M. Detachable photocatalysts of anatase TiO_2 nanoparticles: Annulling surface charge for immediate photocatalyst separation[J]. Appl Surf Sci, 2017, 411: 355-362.

[2] Wu X, Zhao J, Wang L, et al. Carbon dots as solid-state electron mediator for $BiVO_4$/CDs/CdS Z-scheme photocatalyst working under visible light[J]. Appl Catal B: Environ, 2017, 206: 501-509.

[3] Li H, Zheng B, Xue Y, et al. Spray deposited lanthanum doped TiO_2 compact layers as electron selective contact for perovskite solar cells[J]. Sol Energ Mat Sol C, 2017, 168: 85-90.

[4] Qiu Y, Ouyang F, Zhu R. A facile nonaqueous route for preparing mixed-phase TiO_2 with high activity in photocatalytic hydrogen generation[J]. Int J Hydrogen Energ, 2017, 42(16): 11364-11371.

[5] Yu C, Wu Z, Liu R, et al. Novel fluorinated Bi_2MoO_6 nanocrystals for efficient photocatalytic removal of water organic pollutants under different light source illumination[J]. Appl Catal B: Environ, 2017, 209: 1-11.

[6] Wang G, Eastham N D, Aldrich T J, et al. Photoactive blend morphology engineering through systematically tuning aggregation in all-polymer solar cells[J]. Adv Energy Mater, 2018, 8:1702173.

[7] Hsiao Y, Wu T, Wang Y, et al. Evaluating the sensitizing effect on the photocatalytic decoloration of dyes using anatase-TiO_2[J]. Appl Catal B: Environ, 2014(148/149): 250-257.

[8] Le T T, Akhtar M S, Park D M, et al. Water splitting on Rhodamine-B dye sensitized Co-doped TiO_2 catalyst under visible light[J]. Appl Catal B: Environ, 2012, 111-112: 397-401.

[9] Yan X, Xue C, Yang B, et al. Novel three-dimensionally ordered macroporous Fe^{3+}-doped TiO_2 photocatalysts for H_2 production and degradation applications[J]. Appl Surf Sci, 2017, 394:248-257.

[10] Gao M, Zhang D, Pu X, et al. Combustion Synthesis and Enhancement of BiOCl by Doping Eu^{3+} for Photodegradation of Organic Dye[J]. J Am Ceram Soc, 2016, 99(3): 881-887.

[11] 刘建秀,张大凤,蒲锡鹏. $Zn_{0.5}Cd_{0.5}S$:Eu^{3+}半导体材料的燃烧法制备及发光性能研究[J]. 聊城大学学报(自然科学版), 2014, 27(2): 56-59.

[12] Mihai S, Cursaru D L, Ghita D, et al. Morpho ierarhic TiO_2 with plasmonic gold decoration for highly active photocatalysis properties[J]. Mater Lett, 2016, 162: 222-225.

[13] 刘建秀,张彤彤,张大凤,等. Ag 的掺杂量对 $Zn_{0.5}Cd_{0.5}S$/Ag 半导体材料光催化性能的影响[J]. 聊城大学学报(自然科学版), 2015, 28:34-36.

[14] Altın O, Sökmen M, Bıyıklıoğlu Z. Sol gel synthesis of cobalt doped TiO_2 and its dye sensitization for efficient pollutant removal[J]. Mat Sci Semicon Proc, 2016, 45: 36-44.

[15] Xia Y, Li Q, Lv K, et al. Heterojunction construction between TiO_2 hollowsphere and $ZnIn_2S_4$ flower for photocatalysis application [J]. Appl Surf Sci, 2017, 398: 81-88.

[16] Zhang T, Shao X, Zhang D, et al. Synthesis of direct Z-scheme g-C_3N_4/$Ag_2VO_2PO_4$ photocatalysts with enhanced visible light photocatalytic activity[J]. Sep Purif Technol, 2018, 195:332-338.

[17] 邓立成,夏继华,张大凤,等. $Cd_2Nb_2O_7$基光催化材料的水热合成及性能研究[J]. 聊城大学学报(自然科学版),2017,30(4):33-36.

[18] Qi Y L, Zheng Y F, Yin H Y, et al. Enhanced visible light photocatalytic activity of AgBr on {001} facets exposed to BiOCl[J]. J Alloys Compd, 2017, 712: 535-542.

[19] Li J, Zhao K, Yu Y, et al. Facet-Level Mechanistic Insights into General Homogeneous Carbon Doping for Enhanced Solar-to-Hydrogen Conversion[J]. Adv Funct Mater, 2015, 25(14): 2189-2201.

[20] Li K, Liang Y, Yang J, et al. Controllable synthesis of {001} facet dependent foursquare BiOCl nanosheets: A high efficiency photocatalyst for degradation of methyl orange[J]. J Alloys Compd, 2017, 695: 238-249.

[21] 梁姝慧,张大凤,蒲锡鹏. 水解温度对 BiOCl 光催化性能的影响规律研究[J]. 聊城大学学报(自然科学版), 2017, 30(3): 47-50.

[22] Yu N, Chen Y, Zhang W, et al. Preparation of Yb^{3+}/Er^{3+} co-doped BiOCl sheets as efficient visible-light-driven photocatalysts[J]. Mater Lett, 2016, 179: 154-157.

[23] Han X, Dong S, Sun J, et al. Incorporation of Sn-doped BiOCl with reduced graphene oxide for enhanced natural sunlight photocatalysis[J]. Mater Lett, 2017, 187: 154-157.

[24] Yu L, Zhang X, Li G, et al. Highly efficient $Bi_2O_2CO_3$/BiOCl photocatalyst based on heterojunction with enhanced dye-sensitization under visible light[J]. Appl Catal B: Environ, 2016, 187: 301-309.

[25] Mao X, Fan C, Wang Y, et al. RhB-sensitized effect on the enhancement of photocatalytic activity of BiOCl toward bisphenol-A under visible light irradiation[J]. Appl Surf Sci, 2014, 317: 517-525.

[26] LiW T, Huang W Z, Zhou H, et al. Synthesis of Zn^{2+} doped BiOCl hierarchical nanostructures and their exceptional visible light photocatalytic properties[J]. J Alloys Compd, 2015, 638: 148-154.

[27] Cao C, Xiao L, Chen C, et al. Synthesis of novel Cu_2O/BiOCl heterojunction nanocomposites and their enhanced photocatalytic activity under visible light[J]. Appl Surf Sci, 2015, 357(Part A): 1171-1179.

[28] Fitri M A, Ota M, Hirota Y, et al. Fabrication of TiO_2-graphene photocatalyst by direct chemical vapor deposition and its anti-fouling property[J]. Mater Chem Phys, 2017, 198: 42-48.

[29] He J, Wang J, Liu Y, et al. Microwave-assisted synthesis of BiOCl and its adsorption and photocatalytic activity[J]. Ceram Int, 2015, 41(6): 8028-8033.

[30] Ning X, Ge S, Wang X, et al. Preparation and photocathodic protection property of Ag_2S-TiO_2 composites[J]. J Alloys Compd, 2017, 719: 15-21.

[31] Gao Y, Pu X, Zhang D, et al. Combustion synthesis of graphene oxide-TiO_2 hybrid materials for photodegradation of methyl orange [J]. Carbon, 2012, 50(11): 4093-4101.

[32] Hao L, Huang H, Guo Y, et al. Bismuth oxychloride homogeneous phasejunction BiOCl/$Bi_{12}O_{17}Cl_2$ with unselectively efficient photocatalytic activity and mechanism insight[J]. Appl Surf Sci, 2017, 420: 303-312.

[33] Chen X, Mao S S. Titanium Dioxide Nanomaterials: Synthesis, Properties, Modifications, and Applications[J]. Chem Rev, 2007, 107(7): 2891-2959.

[34] Kudo A, Miseki Y. Heterogeneous photocatalyst materials for water splitting[J]. Chem Soc Rev, 2009, 38(1): 253-278.

[35] Lv D, Zhang D, Pu X, et al. One-pot combustion synthesis of $BiVO_4$/BiOCl composites with enhanced visible-light photocatalytic properties[J]. Sep Purif Technol, 2017, 174:97-103.

[36] Yu Y, Cao C, Liu H, et al. A Bi/BiOCl heterojunction photocatalyst with enhanced electron-hole separation and excellent visible light photodegrading activity[J]. J Mater Chem A, 2014, 2(6): 1677-1681.

[37] Chen J, Mei W, Huang Q, et al. Highly efficient three-dimensional flower-like AgI/$Bi_2O_2CO_3$ heterojunction with enhanced photocatalytic performance[J]. J Alloys Compd, 2016, 688: 225-234.

罗丹明敏化 BiOCl 宽光谱响应光催化剂的制备及对苯酚的降解性能研究

杨雅楠 曾甜甜 何银娜 张大凤 蒲锡鹏 马惠彦

(聊城大学 材料科学与工程学院,山东 聊城 252059)

摘 要 采用水解法,通过加入不同量的 NaOH 控制水解反应速率,获得了具有不同形貌的 BiOCl 光催化剂. 用 X 射线粉末衍射、扫描电子显微镜、紫外可见分光光度计和发光光谱表征了材料的结构、形貌和光学性能. 实验结果表明,NaOH 的加入可以减小 BiOCl 的晶粒尺寸,更多量 NaOH 加入时 BiOCl 会严重团聚. 在 23 mmol NaOH 加入时所得 BiOCl 对罗丹明(RhB)的吸附能力和可见光催化能力最好. RhB 敏化显著扩展了 BiOCl 的光谱响应范围. 在可见光激发下,与纯的 BiOCl 相比,敏化后的 BiOCl 对苯酚表现出优异的降解性能,这表明敏化在光催化反应中起到了重要作用. 另外,本文也给出了主要的活性物种和光催化机制.

关键词 氯氧化铋; 光催化剂; 罗丹明; 敏化; 苯酚

中图分类号 O643.36 **文献标识码** A